567756 IN-39
271102
14P.

NASA Contractor Report 185196

Application of Finite-Element-Based Solution Technologies for Viscoplastic Structural Analyses

V.K. Arya
University of Toledo
Toledo, Ohio

March 1990

Prepared for
Lewis Research Center
Under Cooperative Agreement NCC3-120

NASA
National Aeronautics and
Space Administration

APPLICATION OF FINITE-ELEMENT-BASED SOLUTION TECHNOLOGIES FOR VISCOPLASTIC STRUCTURAL ANALYSES

V.K. Arya*
Department of Mechanical Engineering
University of Toledo
Toledo, Ohio 43606

E-5187

SUMMARY

Finite-element solution technology developed for use in conjunction with advanced viscoplastic models is described. The development of such solution technology is necessary for performing stress/life analyses of engineering structural problems where the complex geometries and loadings make the conventional analytical solutions difficult. The versatility of the solution technology is demonstrated by applying it to viscoplastic models possessing different mathematical structures and encompassing isotropic and anisotropic materials. The computational results qualitatively replicate deformation behavior observed in experiments on prototypical structural components.

INTRODUCTION

The drive to enhance and improve the high-temperature performance of structural components used in aerospace and nuclear industries has created a need for the development of realistic viscoplastic models, accompanied by appropriate solution technologies for stress/life analyses of these components. The observed interaction between creep and plastic deformation at high temperatures has led to the development of a number of viscoplastic models. These models treat all inelastic strain as a single time-dependent quantity, and thus automatically include creep, relaxation, and plasticity interactions.

Viscoplastic models are intended to provide realistic descriptions of high-temperature, time-dependent, inelastic behavior of materials. Their mathematical structure is, however, very complex. The highly nonlinear and mathematically "stiff" nature of the constitutive equations makes closed-form analytical solutions virtually impossible. It is, therefore, of the utmost importance that suitable finite-element or other numerical-solution technologies be developed to make these models adaptable for realistic structural and life analyses of these components.

Researchers at the NASA Lewis Research Center have undertaken this important and challenging task. As a result of concerted efforts at NASA Lewis during the last few years, several such solution technologies (in conjunction with the finite-element program MARC and other nonlinear structural analysis codes) have been developed and successfully applied to the solution of a number of uniaxial and multiaxial problems.

This report illustrates the application of some of these solution technologies with regard to the viscoplastic models developed by Robinson, Freed, and

---

*NASA Resident Research Associate at Lewis Research Center.

Dame and Stouffer (refs. 1 to 3). These models have different mathematical structures and encompass both isotropic and anisotropic materials. The intent of this work is to familiarize the researchers and designers in industry with the applicability of these technologies to structural engineering problems. It is expected that the results from the present work will stimulate the use of realistic viscoplastic models for better and more rational component designs.

FINITE-ELEMENT SOLUTION TECHNOLOGY

The finite-element analyses for the uniaxial and multiaxial problems were performed by using the finite-element program MARC (ref. 4). The program has been developed expressly for nonlinear structural analyses and is well equipped with sophisticated computational algorithms and advanced finite-element formulations. The details of the finite-element solution technology developed for use in conjunction with Robinson's model are given in reference 5. The technologies for the other models follow essentially the same structure and can easily be developed. The nonlinear constitutive relationships of the viscoplastic models are implemented through the user subroutine HYPELA. The stiff nature of the constitutive equations requires smart and efficient time-integration strategies for their integration. The integration strategy employed for the present computations is described in the next section.

INTEGRATION STRATEGY

The nonlinear and mathematically stiff nature of the constitutive equations of viscoplastic models calls for special strategies for their integration. This requirement has long been recognized by researchers. As a result, numerous integration strategies that employ either the implicit integration methods (refs. 6 to 12) or the explicit integration methods (refs. 6, 10, 13-15) have been proposed. Since the use of an explicit integration strategy does not require evaluating or inverting a Jacobian matrix, the Euler forward method with an automatic time-step size was used in the present work. A detailed account of various explicit automatic time-step integration strategies is given in references 13 and 15.

The integration strategy used herein can be summarized as follows:

Consider the equation

$$\frac{dy}{dt} = F(y,t) \tag{1}$$

For the solution at time $t + \Delta t$ to be obtained from the known solution at time t, the following steps are required.

(1) Choose a suitable time step (such as Δt). Denote the value of y obtained with this time step as $Y_I (= y_{t+\Delta t})$.

(2) Halve the time step Δt. Denote the value of y (obtained in two steps) as Y_{II} $(= y_{t+\Delta t})$.

(3) Define the tolerance as

$$\mathrm{Tol} = \frac{|y_I - y_{II}|}{|y_{II}|}$$

The upper and lower limits for Tol are prescribed and denoted by Tol_u and Tol_ℓ, respectively. The strategy now runs as follows:

(4) If $\mathrm{Tol} > \mathrm{Tol}_u$, replace Δt by $\Delta t/2$. Go to step (1). Recompute Tol by repeating steps (1) to (3). Repeat the procedure until a time step Δt such that $\mathrm{Tol} < \mathrm{Tol}_u$ is obtained. Accept the corresponding value of y as the value $y_{t+\Delta t}$.

(5) Compare Tol with Tol_ℓ. If $\mathrm{Tol}_\ell > \mathrm{Tol}$, double the time step as used in step (4). If $\mathrm{Tol}_\ell < \mathrm{Tol}$, retain the time step as used in step (4) for the next step calculations.

(6) Continue the computations with the time step rendered by step (5), and so on.

The strategy is easy to implement and works well even for problems with complex geometries and loadings. It can easily be generalized for a system of equations by using concepts (such as defining the error norms) similar to those given in references 13 and 15.

ROBINSON'S MODEL

The viscoplastic model developed by Robinson utilizes the concept of yield surface. The form of model used in the present work has only one state variable, namely, the back stress variable. The yield stress variable is assumed to be constant. The flow law, evolutionary law, and material constants for 2-1/4Cr-1Mo steel can be found in reference 1. The viscoplastic model was implemented in the MARC program and the details of implementation are available in reference 5. Several uniaxial and multiaxial problems were analyzed to demonstrate the feasibility and applicability of the implementation as a useful structural analysis tool. Some representative results are presented below.

A comparison of MARC and experimental hysteresis loops for the alloy 2-1/4Cr-1Mo steel at two strain rates is presented in figure 1. Excellent agreement is observed between the MARC and experimental loops. Such uniaxial calculations (both here and in the case of other viscoplastic models) and their comparison with the experimental data are done in order to validate the finite-element implementation of the model and to gain confidence in applying it to complex and computationally intensive problems.

As an application of the finite-element solution technology developed at NASA Lewis to an engineering structural problem, a nonlinear structural analysis was performed for an actively cooled cowl lip (the name given to the structural leading edge of an engine inlet of a proposed hypersonic aircraft). This structural component is subject to severe thermal loadings and gradients during simulated flight. The three-dimensional finite-element model (shown in fig. 2) and the calculated steady-state temperatures on the cowl lip were taken from the work of Melis and Gladden (ref. 16). The material of the cowl lip was assumed to be a copper-based alloy NARloy-Z. The constants for this material were obtained from Robinson and Arnold (ref. 17). The thermal loading cycle used in numerical computations is shown in figure 3.

Figures 4 to 6 show the stress and strain distributions in the cowl lip. The stress and total strain distributions along the edge of the cowl lip at 0.75 sec are shown in figures 4 and 5, respectively. The total (mechanical) strain in figure 5 is the sum of elastic and inelastic strains. From figure 5 the largest total strain is observed to occur along the edge of the cowl lip. Figure 6 displays the stresses at 2.25 sec. It is interesting to note that the elastic-viscoplastic analysis is capable of capturing the redistribution of stress during even a small period of steady-state thermal loading, that is, between 0.75 and 2.25 sec. This redistribution of stress with time is evident on comparing figure 4 with figure 6. The elastic-plastic-creep analysis in reference 18 was unable to depict this redistribution of stress with time.

FREED'S VISCOPLASTIC MODEL

Freed's model incorporates two internal state variables, namely, the back stress and drag stress. The tensorial back stress accounts for strain-induced kinematic hardening, whereas the isotropic hardening in the model is included via the scalar drag stress. A small displacement and a small strain formulation are employed. It is assumed that there is no coupling between the static and dynamic recovery terms in the evolutionary equations for the state variables. This imparts a simpler mathematical framework for the model. The flow law, evolutionary laws, and values of the constants for copper for this model can be found in reference 2. The model was implemented in the MARC program, and several uniaxial problems and a cylindrical thrust chamber nozzle problem were analyzed by using this finite-element implementation. The uniaxial loadings shown in figure 7 consisted of mechanical and thermal (both isothermal and nonisothermal) loadings. Nonisothermal loadings included both in-phase and out-of-phase loadings.

Stabilized hysteresis loops, calculated from the model, for isothermal and nonisothermal (both in-phase and out-of-phase) loadings are plotted in figures 8 to 10. The strain range is 2.0 percent and the strain rate is 0.001/sec for isothermal loops. For nonisothermal loops, the mechanical strain range is 0.8 percent and the rate is 1.5×10^{-5}/sec. To facilitate comparison, the experimental hysteresis loops are also plotted in these figures. A comparison of these figures reveals good agreement between the experimental and predicted stabilized hysteresis loops obtained with the finite-element implementation. This gives confidence to apply the implementation to a multiaxial nozzle problem.

The finite-element model of the cylindrical rocket nozzle shown in figure 11 and the calculated temperatures and pressure loadings were taken from reference 19. Generalized plane-strain isoparametric elements were used to model the smallest repeating segment of the cylinder wall. Time-varying nodal temperatures and pressure loadings (see ref. 19) were applied to compute chamber wall deformation histories for a number of firing cycles. The nonlinear variations in temperature-dependent material properties were accounted for in the computations.

The deformed geometries of the component after the first and sixth firing cycles are plotted in figure 12. A magnification factor of about 15 was applied to the deformed shape to facilitate the visual interpretation of the results. Also shown is the deformed shape of the component as observed in a cyclic experiment carried to 393 cycles. It is encouraging to note that the analysis qualitatively predicts the progressively deformed shape that results in the "dog-house" effect observed in the experiments.

STOUFFER'S SINGLE-CRYSTAL MODEL

Owing to the presence of grain boundaries, conventionally cast polycrystalline superalloys are susceptible to transverse grain boundary oxidation, corrosion and creep deformation, and subsequent cracking. The absence of grain boundaries in single-crystal alloys such as Rene-N4, MAR-M 247, PWA 1480, and CMSX has made them useful in gas turbine engines. A time-dependent, micromechanics, crystallographic model was developed by Dame and Stouffer (ref. 3) to characterize the inelastic behavior of single-crystal alloys. The model contains only the isotropic state variable. To make the model applicable in the analysis and design of single-crystal components, it was implemented in the MARC program. Several uniaxial problems, including creep, relaxation, and tensile and cyclic loadings, were analyzed.

Predicted and experimental stress-strain curves for the single-crystal alloy Rene-N4 at 1400 °F (760 °C) are plotted in figure 13. The crystal orientations are (1 0 0), (1 1 0) and (9 3 0). Good agreement between predictions using the MARC program and experimental results was observed.

Figure 14 exhibits creep curves at 1400 °F (760 °C) in the (1 0 0) direction. The curves are plotted for three different loadings of 621 MPa (90 ksi), 655 MPa (95 ksi), and 758 MPa (110 ksi). The experimental curves are also plotted to facilitate comparison. Again, good agreement between the predicted and experimental results was obtained.

A comparison of predicted relaxation curves from the present work and the work of Dame and Stouffer (ref. 3) is presented in figure 15. The crystal orientations are (1 0 0) and (1 1 0). The experimental relaxation data for Rene-N4 were unavailable. It is seen that the predicted curves from these two works compare very well.

Figure 16 displays a comparison of MARC calculated and experimental hysteresis loops in the (1 1 0) direction. The strain range is ±0.6 percent and the temperature is 1400 °F (760 °C). Excellent agreement between the predicted and experimental hysteresis loops confirmed the correct finite-element implementation of the single-crystal constitutive model. It gives the confidence to apply this finite-element implementation to more complex loading conditions of more complex geometries. The results of such analyses will be reported subsequently.

CONCLUSIONS

Numerical-solution technology employing the finite-element method was developed to perform the nonlinear structural analyses with viscoplastic models. The technology is illustrated for three models but is general in nature. Several uniaxial problems and a multiaxial problem were analyzed. Good agreement between the experimental and predicted hysteresis loops for uniaxial thermomechanical loadings confirms the correct finite-element implementation of the viscoplastic models. Finite-element analyses were performed for the multiaxial problems by using the "validated" implementation. It is seen that viscoplastic models are capable of describing thermal/mechanical phenomena observed in the experiments. The versatility of the finite-element solution technology developed herein is demonstrated by successful application to three different types of viscoplastic models.

REFERENCES

1. Robinson, D.N.; and Swindeman, R.W.: Unified Creep-Plasticity Constitutive Equations for 2-1/4Cr-1Mo Steel at Elevated Temperature. ORNL/TM-8444, 1982.

2. Freed, A.D.; and Verrilli, M.J.: A Viscoplastic Theory Applied to Copper. NASA TM-100831, 1988.

3. Dame, L.T.; and Stouffer, D.C.: Anisotropic Constitutive Model for the Nickel Base Single-Crystal Alloys: Development and Finite Element Implementation. NASA CR-175015, 1986.

4. MARC General-Purpose Finite Element Program. MARC Research Analysis Research Corporation, Palo Alto, CA, 1983.

5. Arya, V.K.; and Kaufman, A.: Finite Element Implementation of Robinson's Viscoplastic Model and its Application to Some Uniaxial and Multiaxial Problems. NASA TM-89891, 1987.

6. Arnold, S.M.: Effects of State Recovery on Creep Buckling Induced by Thermomechanical Loading. Ph.D. Thesis, Akron University, 1987.

7. Walker, K.P.: A Uniformly Valid Asymptotic Integration Algorithm for Unified Viscoplastic Constitutive Models. Advances in Inelastic Analysis, AMD-Vol. 88, S. Nakazawa, K. Willain, and N. Rebelo, eds., ASME, 1987, pp. 13-27.

8. Freed, A.D.; and Walker, K.P.: Refinements in a Viscoplastic Model. NASA TM-102338, 1989.

9. Chulya, A.; and Walker, K.P.: A New Uniformly Valid Asymptotic Integration Algorithm for Elasto-Plastic-Creep and Unified Viscoplastic Theories Including Continuum Damage. NASA TM-102344, 1989.

10. Saleeb, A.F., et al.: On Finite Element Implementation and Computational Techniques for Constitutive Modeling of High Temperature Composites. NASA CR-185120, 1989.

11. Cordts, D.; and Kollmann, F.G.: An Implicit Time Integration Scheme for Inelastic Constitutive Equations with Internal State Variables. Int. J. Numer. Methods Eng., vol. 23, no. 4, 1986, pp. 533-554.

12. Hornberger, K.; and Stamm, H.: An Implicit Integration Algorithm with a Projection Method for Viscoplastic Constitutive Equations. Int. J. Numer. Methods Eng., vol. 28, no. 10, Oct. 1989, pp. 2397-2421.

13. Arya, V.K.; Hornberger, K.; and Stamm, H.: On the Numerical Integration of Viscoplastic Models. KfK-4082, 1986.

14. Cassenti, B.N.: Research and Development Program for the Development of Advanced Time-Temperature Dependent Constitutive Relationships. Vols. 1-2, (R83-956077-1,-2, United Technologies Research Center; NASA Contract NAS3-23273) NASA CR-168191-VOL-1,-VOL-2, 1983.

15. Kumar, V.; Morjaria, M.; and Mukherjee, S.: Numerical Integration of Some Stiff Constitutive Models of Inelastic Deformation. J. Eng. Mater. Technol., vol. 102, no. 1., Jan. 1980, pp. 92-96.

16. Melis, M.E.; and Gladden, H.J.: Thermostructural Analysis with Experimental Verification in a High Heat Flux Facility of a Simulated Cowl Lip. 29th Structures, Structural Dynamics and Materials Conference, Part 1, AIAA, 1988, pp. 106-115.

17. Robinson, D.N.; and Arnold, S.M.: Effects of State Recovery on Creep Buckling Under Variable Loading. NASA CR-175094, 1986.

18. Arya, V.K.; Melis, M.E.; and Halford, G.R.: A Finite Element Elastic-Plastic-Creep and Cyclic Life Analysis of a Cowl Lip. NASA TM-102342, 1989.

19. Quentmeyer, R.J.: Thrust Chamber Thermal Barrier Coating Techniques. NASA TM-100933, 1988.

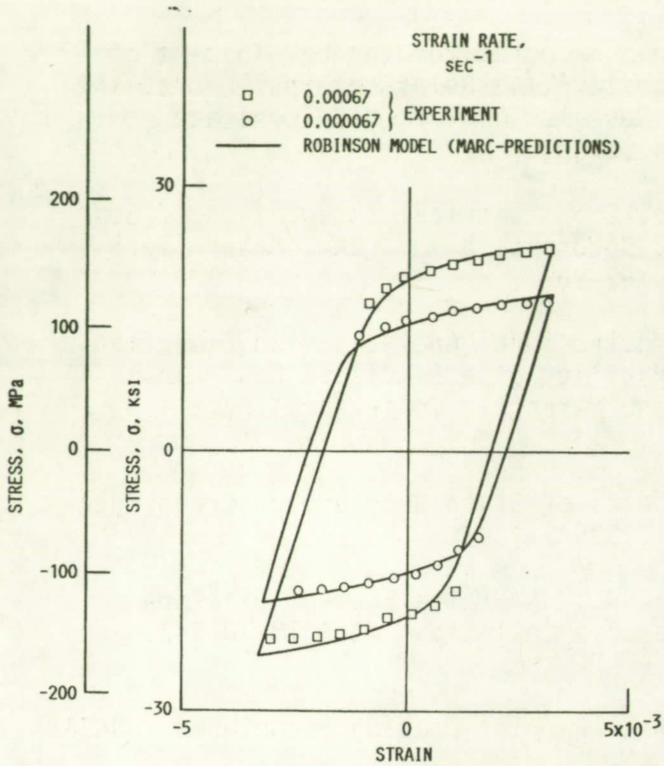

FIGURE 1. - STABILIZED HYSTERESIS LOOPS FOR 2-1/4 Cr-1 Mo STEEL AT 538 °C (1000 °F). EXPERIMENTAL RESULTS TAKEN FROM ROBINSON AND SWINDEMAN (REF. 1).

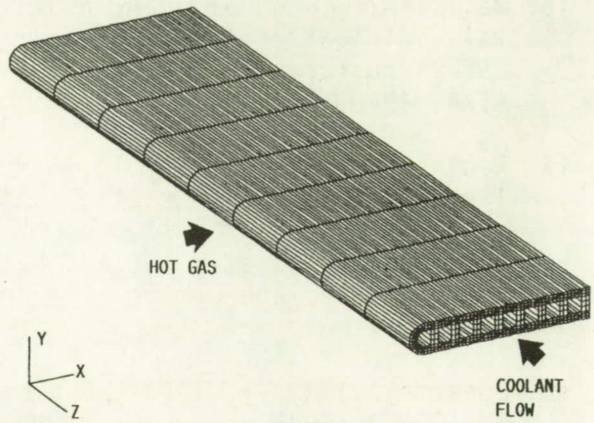

FIGURE 2. - COWL LIP FINITE-ELEMENT MODEL. ELEMENTS, 3294; NODES, 4760.

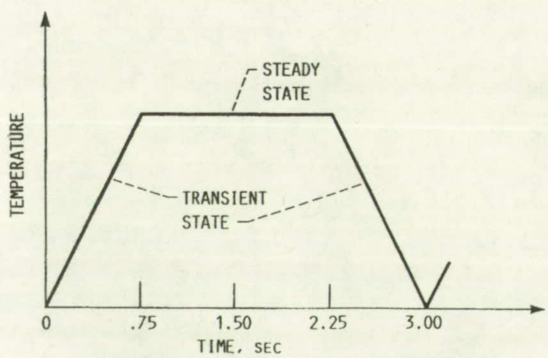

FIGURE 3. - THERMAL LOADING CYCLE FOR COWL LIP PROBLEM.

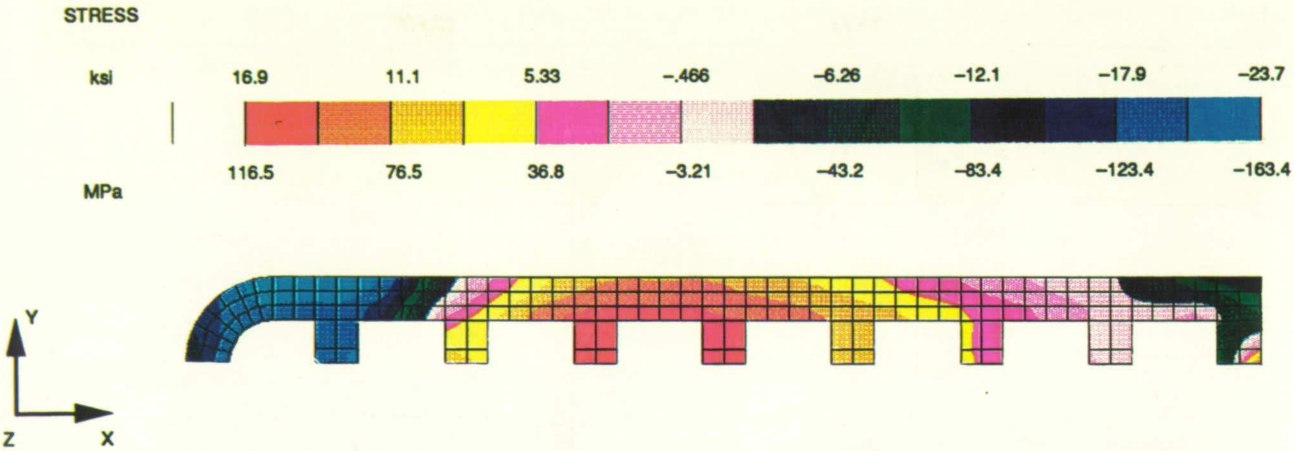

FIGURE 4. - STRESS IN Z-DIRECTION IN COWL LIP; ELASTIC-VISCOPLASTIC ANALYSIS (ROBINSON'S MODEL). TIME, 0.75 sec; CROSS FLOW, GH_2 COOLANT.

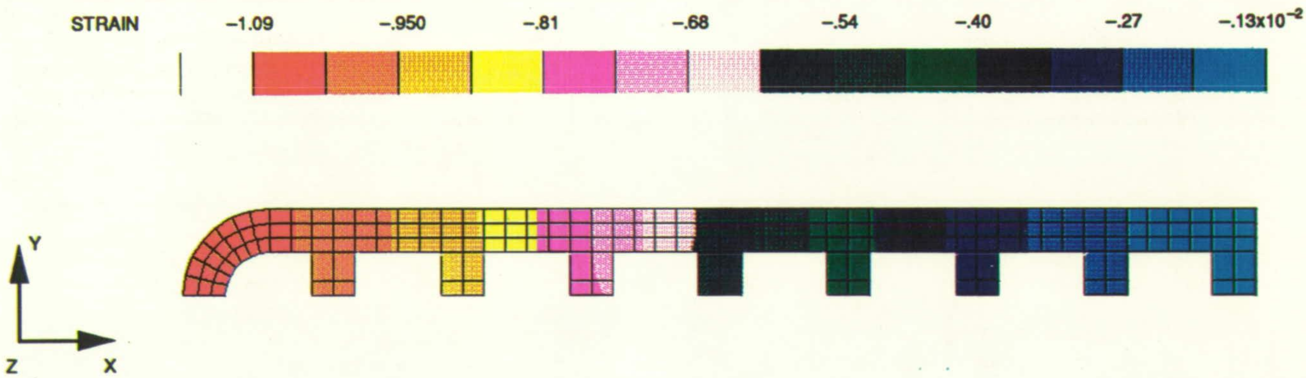

FIGURE 5. - TOTAL STRAIN IN Z-DIRECTION IN COWL LIP; ELASTIC-VISCOPLASTIC ANALYSIS (ROBINSON'S MODEL). TIME, 0.75 sec; CROSS FLOW, GH_2 COOLANT.

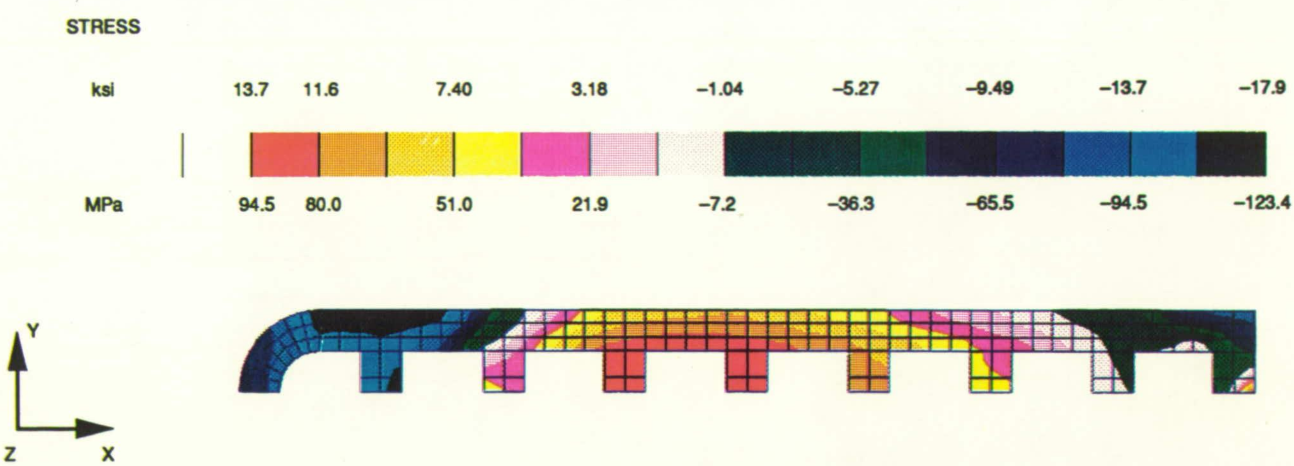

FIGURE 6. - STRESS IN Z-DIRECTION IN COWL LIP; ELASTIC-VISCOPLASTIC ANALYSIS (ROBINSON'S MODEL). TIME, 2.25 sec; CROSS FLOW, GH_2 COOLANT.

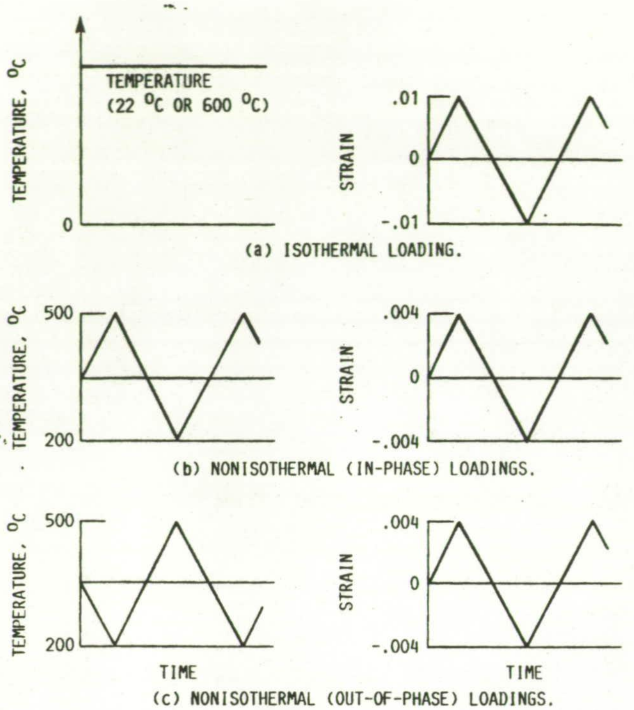

FIGURE 7. - CYCLIC THERMAL AND MECHANICAL LOADING USED TO GENERATE HYSTERESIS LOOPS BY THE MARC FINITE-ELEMENT CODE FOR FREED'S MODEL.

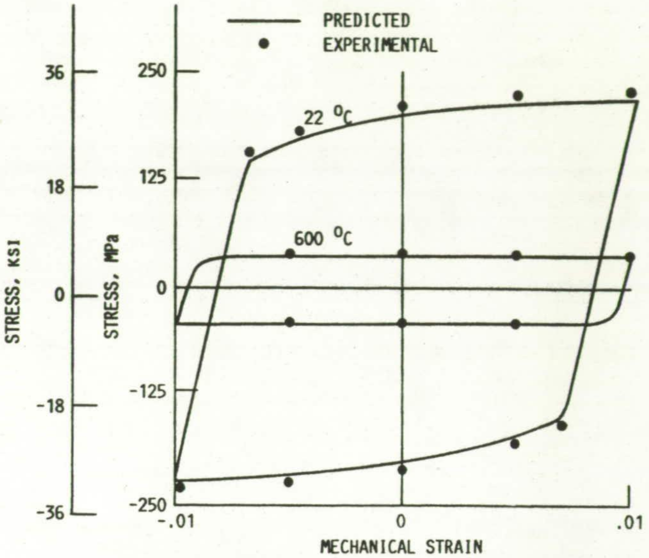

FIGURE 8. - PREDICTED STABILIZED HYSTERESIS LOOPS USING FREED'S MODEL (ISOTHERMAL LOADING). EXPERIMENTAL DATA FROM FREED AND VERRILLI (1988). STRAIN RATE, 0.001/SEC.

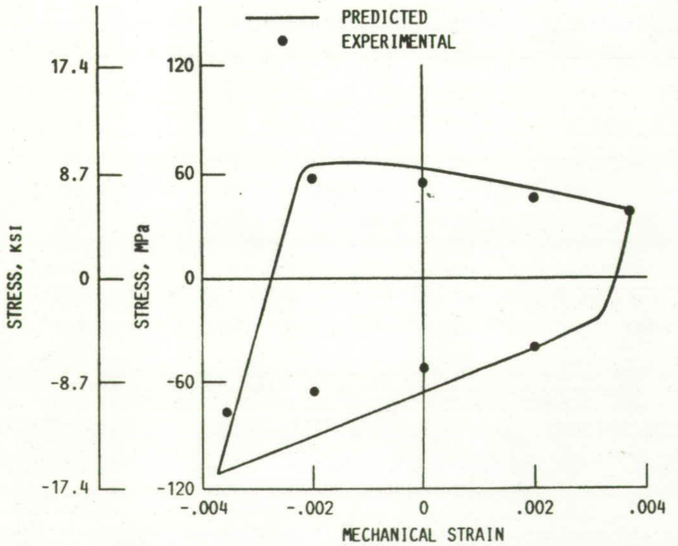

FIGURE 9. - IN-PHASE PREDICTED HYSTERESIS LOOPS FOR COPPER USING FREED'S MODEL. EXPERIMENTAL DATA FROM FREED AND VERRILLI (1988). TEMPERATURE, 200 ⇄ 500 °C; STRAIN RATE, 1.5×10^{-5}/SEC.

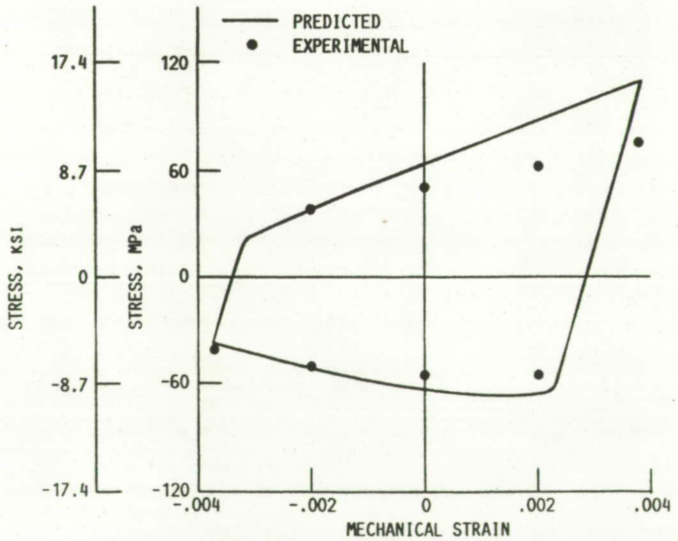

FIGURE 10. - OUT-OF-PHASE PREDICTED HYSTERESIS LOOPS FOR COPPER USING FREED'S MODEL. EXPERIMENTAL DATA FROM FREED AND VERRILLI (1988). TEMPERATURE, 200 ⇄ 500 °C; STRAIN RATE, 1.5×10^{-5}/SEC.

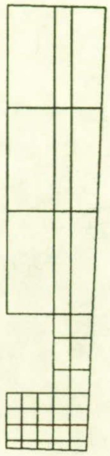

FIGURE 11. - CYLINDRICAL ROCKET NOZZLE FINITE-ELEMENT MODEL. ELEMENTS, 35; NODES, 54.

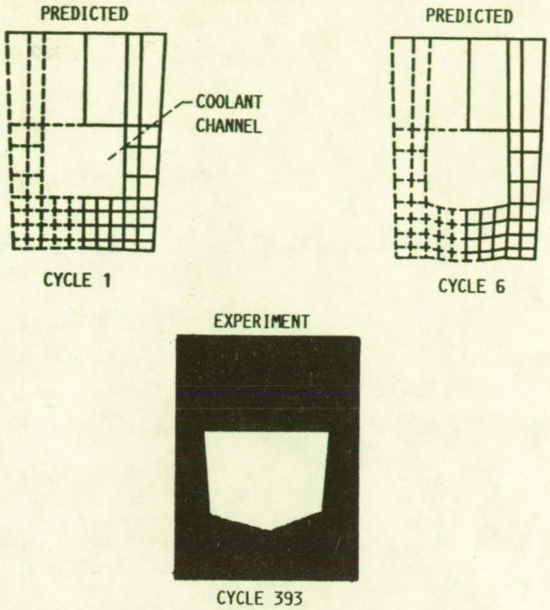

FIGURE 12. - PROGRESSIVE SHAPE OF COMPONENT. PLOT MAGNIFICATION FACTOR, ≈ 15.

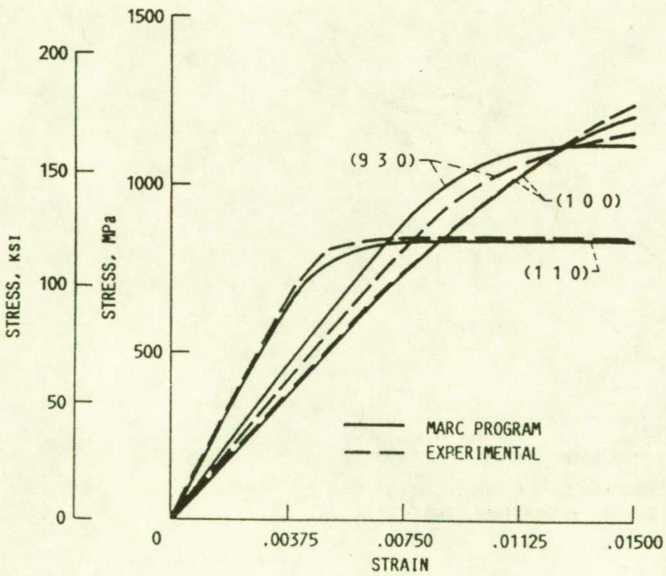

FIGURE 13. - STRESS-STRAIN CURVES FOR SINGLE-CRYSTAL ALLOY (RENE-N4). TEMPERATURE, 760 °C (1400 °F).

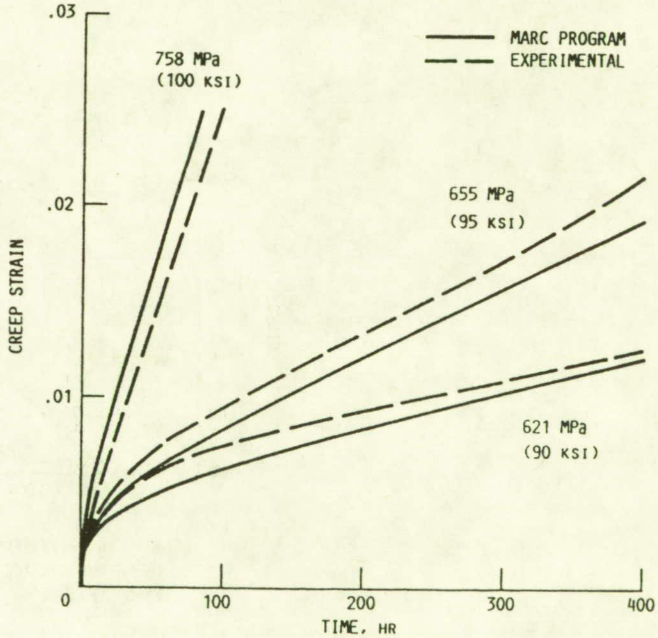

FIGURE 14. - CREEP CURVES FOR SINGLE-CRYSTAL ALLOY (RENE-N4). DIRECTION (1 0 0); TEMPERATURE, 760 °C (1400 °F).

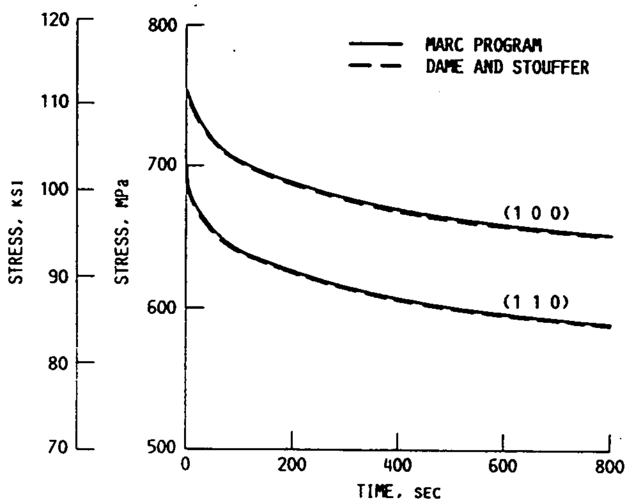

FIGURE 15. - RELAXATION CURVES FOR SINGLE-CRYSTAL ALLOY (RENE-N4). TEMPERATURE, 760 °C (1400 °F).

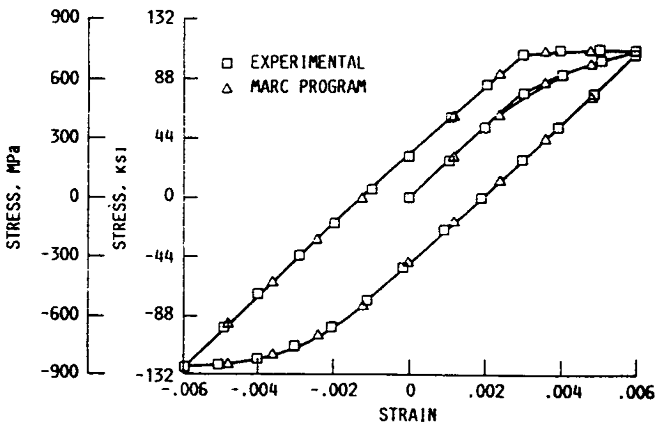

FIGURE 16. - HYSTERESIS LOOPS FOR SINGLE-CRYSTAL ALLOY (RENE-N4). DIRECTION (1 1 0); TEMPERATURE, 760 °C (1400 °F).

NASA
National Aeronautics and Space Administration

Report Documentation Page

1. Report No. NASA CR-185196	2. Government Accession No.	3. Recipient's Catalog No.
4. Title and Subtitle Application of Finite-Element-Based Solution Technologies for Viscoplastic Structural Analyses		5. Report Date March 1990
		6. Performing Organization Code
7. Author(s) V.K. Arya		8. Performing Organization Report No. None (E-5187)
		10. Work Unit No. 510-01-01
9. Performing Organization Name and Address University of Toledo, Department of Mechanical Engineering, Toledo, Ohio 43606		11. Contract or Grant No. NCC3-120
		13. Type of Report and Period Covered Contractor Report Final
12. Sponsoring Agency Name and Address National Aeronautics and Space Administration, Lewis Research Center, Cleveland, Ohio 44135-3191		14. Sponsoring Agency Code

15. Supplementary Notes

Project Manager, Gary Halford, Structures Division, NASA Lewis Research Center. V.K. Arya, University of Toledo and NASA Resident Research Associate at Lewis Research Center.

16. Abstract

Finite-element solution technology developed for use in conjunction with advanced viscoplastic models is described. The development of such solution technology is necessary for performing stress/life analyses of engineering structural problems where the complex geometries and loadings make the conventional analytical solutions difficult. The versatility of the solution technology is demonstrated by applying it to viscoplastic models possessing different mathematical structures and encompassing isotropic and anisotropic materials. The computational results qualitatively replicate deformation behavior observed in experiments on prototypical structural components.

17. Key Words (Suggested by Author(s)) Viscoplasticity; Finite-element analysis; Viscoplastic models; Single-crystal materials; Nonlinear structural analysis	18. Distribution Statement Unclassified – Unlimited Subject Category 39

19. Security Classif. (of this report)	20. Security Classif. (of this page)	21. No. of pages	22. Price*
Unclassified	Unclassified	12	A03

NASA FORM 1626 OCT 86

*For sale by the National Technical Information Service, Springfield, Virginia 22161

National Aeronautics and
Space Administration

Lewis Research Center
Cleveland, Ohio 44135

NASA